Electrochemical and Corrosion Behaviour of a New Titanium Base Alloy in Simulated Human Electrolytes

Cora Vasilescu, Paula Drob, Ecaterina Vasilescu, Petre Osiceanu, Silviu Iulian Drob[*],
Mihai Vasile Popa

Institute of Physical Chemistry "Ilie Murgulescu" of Romanian Academy, Spl. Independentei 202, PO BOX 12-194, 060021 Bucharest, Romania
[*]E-mail: sidrob@chimfiz.icf.ro

A new quaternary alloy Ti-10Nb-10Zr-5Ta with near β fine, homogeneous microstructure, low Young's modulus of 63.4 GPa and better mechanical properties than those of the commercial Ti was obtained. This alloy demonstrated nobler electrochemical behaviour, lower corrosion rates and more favourable long-term behaviour in simulated human electrolytes, Ringer solutions of different pH values that can appear in the human body, in the "working life" of an implant. The alloy native passive film contains (XPS analysis) both Ti_2O_3 and TiO_2 protective oxides and, in addition, the very protective Nb_2O_5, ZrO_2 and Ta_2O_5 oxides which strengthened and reinforced this film. Moreover, this passive film thickened and improved its protective properties in time. Corrosion rates placed the new alloy in the "Very Stable" resistance class and the corresponding lower ion release rates represent more reduced quantities of ions released into surrounding tissues in comparison with Ti. Alloy polarisation resistances had ten times higher values than those of Ti, indicating a more compact, barrier, resistant passive layer. Nyquist spectra showed that the new alloy presented higher capacitive, protective film than that of Ti. Bode spectra revealed two phase angles, indicative of a bi-layered passive film that was modelled with an electric equivalent circuit with two time constants: the first time constant.

1. INTRODUCTION

In the last decade, the necessity of the properly improvement of the implant alloys is stringently because these alloys must combine good mechanical properties with very good corrosion resistance in the physiological fluid and biocompatibility. Firstly, the implant alloys must contain only non-toxic and non-allergic elements: Ti, Nb, Zr, Ta, Pt, Pd, Sn [1, 2]. Secondly, these alloys must possess a low Young's modulus to prevent the stress shield; this requirement can be realised by the using of Nb, Ta,

and Zr elements that conduct to alloys with β or near β microstructure, reduced modulus and high strength [3, 4]. Ternary and quaternary alloys were developed. The most known ternary alloy is Ti-13Nb-13Zr (ASTM F 1713-96) with a near β microstructure, good corrosion resistance and mechanical properties (Young's modulus of 79 GPa) [5, 6]. Okazaki et al. obtained Ti-15Zr-4Nb-4Ta-0.2Pd-0.2O-0.05N alloy with a Young's modulus of 97 GPa [3, 4, 7, 8], higher than that of the human bone of 30-40 GPa [9]. Also, Banerjee et al. [10] applied different thermal treatments to Ti-34Nb-9Zr-8Ta alloy (Young's modulus of 89 GPa) and a decrease in hardness was indicated. The new Ti-29Nb-13Ta-4.6Zr alloy [11-15] shows a good Young's modulus of 60 GPa but its biocompatibility is inadequate and it lacks bioactivity. The surface of the novel near β alloy, Ti-5Zr-3Sn-5Mo-15Nb [16] with a Young's modulus of 69 GPa was functionalised by microarc oxidation to increase the bone cell adhesion, spread and viability. Porous near β Ti-35Nb-7Zr-5Ta alloy [17, 18] was produced by power metallurgy and had a low Young's modulus of 55 GPa; different treatments were performed and some properties became better and another lower, recommending further detailed investigations.

We proposed a new quaternary alloy Ti-10Nb-10Zr-5Ta with near β fine, homogeneous microstructure, low Young's modulus of 63.4 GPa and better mechanical properties than those of the commercial Ti; also, this alloy demonstrated nobler electrochemical behaviour, lower corrosion rates and more favourable long-term behaviour in simulated human electrolytes, Ringer solutions of different pH values that can appear in the human body, in the "working life" of an implant.

2. EXPERIMENTAL

2.1. Alloy synthesis

The alloy was synthesised by high vacuum, levitation melting and re-melting using pure elements: titanium according to ASTM F 67, niobium 99.81% purity, zirconium 99.6% purity and tantalum 99.59% purity. The alloy composition is presented in Table 1.

Table 1. Alloy composition.

% wt.										
Nb	Zr	Ta	Fe	O	N	H	Si	Mg	Al	Ti
10.18	9.648	4.466	0.0001	0.15	0.03	0.002	0.0013	0.046	0.002	balance

2.2. Determination of alloy microstructure

For the microstructure analysis, the cylindrical samples were grinded with different abrasive paper till 2000 grade, polished on alumina paste till mirror surface and then were chemically etched in a solution of 68% glycerine, 16% HF and 16% HNO_3. The alloy microstructure in as-cast and processed state was analysed with an optical microscope, type AXIO IMAGER A1m.

2.3. Determination of alloy mechanical properties

The tensile tests for as-cast alloy were carried out until fracture using an INSTRON 3382 module. Stress - strain tensile curve was obtained; from this curve, the following main mechanical properties were calculated: Young's modulus (E), ultimate tensile strength (σ_{max}), strain to fracture (ε_f), and 0.2% yield strength ($\sigma_{0.2}$). Three experiments were performed and the reproducibility was very good.

2.4. Determination of alloy corrosion resistance

The alloy corrosion resistance was studied in Ringer solutions of acid, neutral and alkaline pH, simulating the possible severe functional conditions from the human body: the acid pH appears after surgery because the hydrogen concentration increases in the traumatised tissues and by the in time hydrolysis of the surface oxides; the alkaline pH develops in the distress periods of the human body [19-21]. Ringer solution composition was (g/L): NaCl – 6.8; KCl – 0.4; $CaCl_2$ – 0.2; $MgSO_4.7H_2O$ – 0.2048; $NaH_2PO_4.H_2O$ – 0.1438; $NaHCO_3$ – 1; glucose – 1; pH = 7.58; pH = 3.36 was obtained by HCl addition; pH = 8.91 was obtained by KOH addition. Solution temperature was kept at $37^0C \pm 1^0C$.

From as-cast ingots were cut cylindrical samples that firstly were grinded and polished to mirror surface; then, the samples were ultrasonically degreased in acetone and bi-distilled water for 15 min. and mounted in a Stern-Makrides mount system.

The following electrochemical techniques were used: cyclic potentiodynamic and linear polarisation, electrochemical impedance spectroscopy (EIS) and monitoring of the open circuit potentials and corresponding open circuit potential gradients.

The potentiodynamic polarisation was applied from the cathodic (a potential with about 500 mV more electronegative than the open circuit potential, E_{oc}) to the anodic domain (till + 2000 mV vs. SCE) with a scan rate of 1 mV/s; VoltaLab 80 equipment with its VoltaMaster 4 program were used. From the curves, the main electrochemical parameters were determined: E_{corr} – corrosion potential, like zero current potential, E_p – passivation potential at which the current density is constant; $|E_{corr} - E_p|$ difference represents the tendency to passivation (low values characterise a good, easy passivation); ΔE_p – passive potential range of the constant current; j_p – passive current density.

The linear polarisation was carried out to obtain Tafel curves for a potential range of $\pm$ 100 mV around E_{oc}, with a scan rate of 1 mV/sec. The VoltaMaster 4 program directly supplies the corrosion current densities, j_{corr} and rates, V_{corr} and polarisation resistance, R_p [22-24]. The total quantity of ions released into biofluid was calculated [25, 26].

The electrochemical impedance spectroscopy was performed at E_{oc}, [27, 28] with Voltalab 80 equipment; the amplitude of the AC potential was 5 mV and simple sine measurements at frequencies between 0.1 Hz and 10^2 kHz were acquired for each sample. Nyquist and Bode plots were recorded. The electric equivalent circuit was fitted by non-linear, least square program ZVIEW.

The open circuit potentials E_{oc} (vs. SCE) were monitored [29] during an exposure period of 1000 hours till present, using a performing Hewlett-Packard multimeter. Also, the open circuit

potential gradients due to the non-uniformities of the Ringer solutions pH, ΔE_{oc}(pH) were calculated as:

$$\Delta E_{oc1}(pH) = E_{oc}^{pH=3.36} - E_{oc}^{pH=7.58} \tag{1}$$

$$\Delta E_{oc2}(pH) = E_{oc}^{pH=3.36} - E_{oc}^{pH=8.91} \tag{2}$$

$$\Delta E_{oc3}(pH) = E_{oc}^{pH=7.58} - E_{oc}^{pH=8.91} \tag{3}$$

*2.5. Determination of native passive film composition*

The composition of the native passive film was determined by X-Ray Photoelectron Spectroscopy (XPS). Surface analysis was carried out on Quantera SXM equipment with a base pressure in the analysis chamber of $1.33322 \cdot 10^{-7}$ Pa. The X-ray source was Al K_{α} radiation (1486.6 eV, monochromatized) and the overall energy resolution is estimated at 0.75 eV by the full width at half maximum (FWHM) of the Au $4f_{7/2}$ line. In order, to take into account the charging effect on the measured Binding Energies (BEs), the spectra were calibrated using the C 1s line (BE = 284.8 eV, C-C (CH)n bonding) of the adsorbed hydrocarbon on the sample surface. It is appropriate to note here that all the calculations were performed assuming that the samples were homogeneous within the XPS detected volume. The errors in the quantitative analysis (relative concentrations) were estimated in the range of ±10%, while the accuracy for binding energies assignments was ±0.2 eV.

3. RESULTS AND DISCUSSION

3.1. Alloy microstructure

The optical micrographs of the samples (Fig. 1) revealed near β fine, homogeneous, casting dendrite microstructure and a superposed polygonal microstructure as result of the recrystallization of the alloy during the vacuum cooling in the furnace.
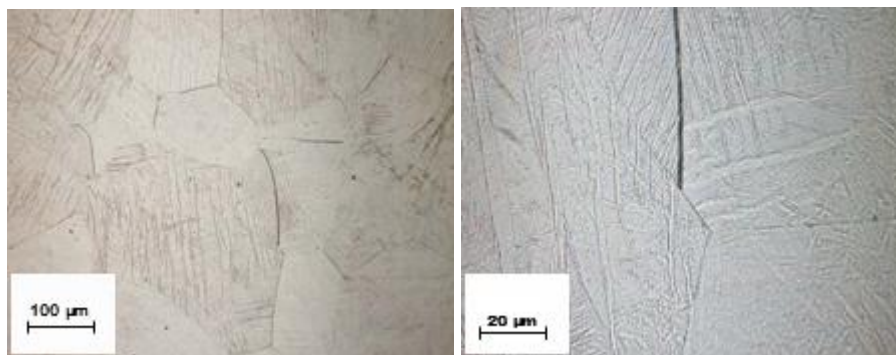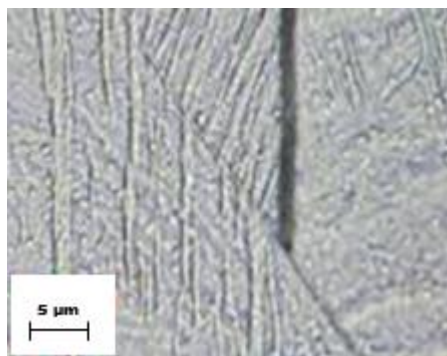
Figure 1. Optical micrographs of Ti-10Nb-10Zr-5Ta alloy at different magnifications.


3.2. Alloy mechanical properties

Figure 2 shows the stress-strain curve and Table 2 summarizes main mechanical properties of as-cast Ti-10Nb-10Zr-5Ta alloy related to those of Ti. The tensile curve indicates elastoplastic behaviour with an initial elastic behaviour. Both, ultimate tensile strength (σ_{max}), strain to fracture (ε_f), and 0.2% yield strength ($\sigma_{0.2}$) have higher values than those of Ti, denoting a good resistance to load bearing conditions. Young's modulus of 63.4 GPa closed to that of the human bone (30-40 GPa) [9] represents a very good value that will not cause the bone atrophy or resorption, assuring a very long "service life time" [30] for the alloy. Moreover, this alloy mechanical properties are more favourable compared with those of others β-type alloys as Ti-15Zr-4Nb-4Ta [10] or Ti-5Zr-3Sn-5Mo-15Nb [16].

Table 2. Main mechanical properties of Ti-10Nb-10Zr-5Ta alloy.

| Material	E (GPa)	σ_{max} (MPa)	ε_f (%)	$\sigma_{0.2}$ (MPa)
Ti*	105.0	344.0	20.0	170-244
Ti-10Nb-10Zr-5Ta	63.47	738.18	23.24	221.12

*ASM data base
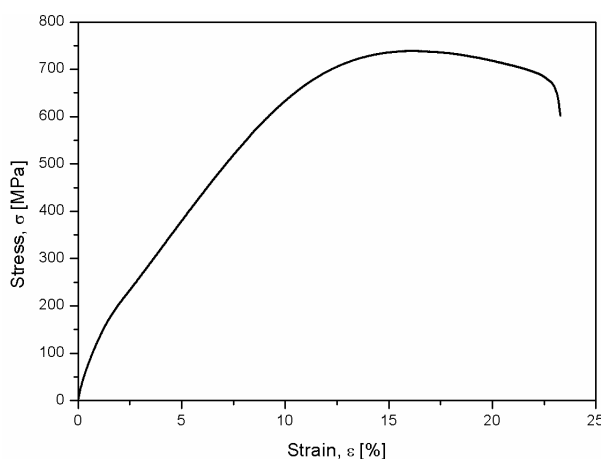
Figure 2. Stress-strain tensile curve for Ti-10Nb-10Zr-5Ta alloy.

3.3. Alloy electrochemical and corrosion behaviour in simulated human electrolytes

3.3.1. Alloy electrochemical behaviour from cyclic polarisation curves

Figure 3 shows the comparison of the cyclic polarisation curves between Ti-10Nb-10Zr-5Ta alloy and Ti; the polarisation curves immediately entered the passive zone; the polarisation patterns indicated a difference between those two materials: the alloy exhibited lower passive current densities representing an excellent corrosion resistance [7]; also, the alloy passive current densities remained constantly with increasing potential that reveal the thickening of its passive layer [14].
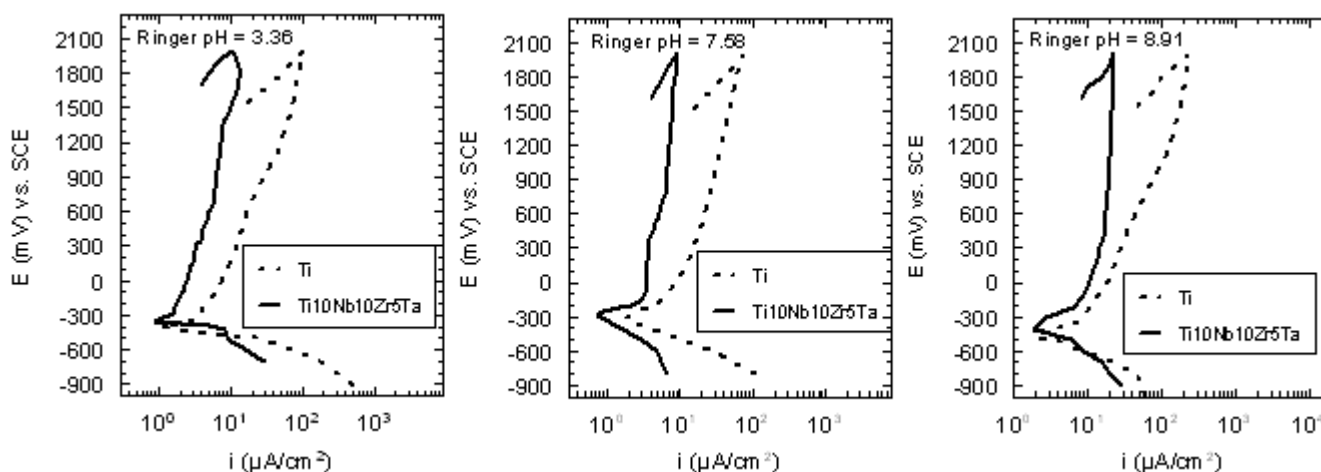
Figure 3. Anodic cyclic potentiodynamic curves for Ti-10Nb-10Zr-5Ta alloy in comparison with those of Ti in Ringer solutions, at 37^0C.

The corrosion potential, E_{corr} (Table 3) shifted to more anodic values due to the formation of a relatively more compact film on the alloy surface [23] that contains both Ti_2O_3 and TiO_2 protective oxides and in addition Nb_2O_5, ZrO_2, and Ta_2O_5 protective oxides (as will be demonstrated by XPS analysis); these oxides strengthened the alloy passive film.

Table 3. Main electrochemical parameters obtained for Ti-10Nb-10Zr-5Ta alloy in comparison with those of Ti in Ringer solutions, at 37^0C

Material	E_{corr} (mV)	E_p (mV)	ΔE_p (mV)	$|E_{corr} - E_p|$ (mV)	j_p ($\mu A/cm^2$)
Ringer pH = 3.36					
Ti	-400	-100	>2000	300	25
Ti-10Nb-10Zr-5Ta	-350	-200	>2000	200	4.2
Ringer pH = 7.58					
Ti	-320	-50	>2000	270	15
Ti-10Nb-10Zr-5Ta	-280	-150	>2000	130	3.7
Ringer pH = 8.91					
Ti	-500	-200	>2000	300	18
Ti-10Nb-10Zr-5Ta	-400	-200	>2000	200	10.5

The composition of the native passive film on the Ti-10Nb-10Zr-5Ta alloy surface was determined by X-ray photoelectron spectroscopy (XPS). The survey spectrum (Fig. 4) displayed the presence of Ti 2p, Nb 3d, Zr 3d, Ta 4f and O 1s [11, 31, 32]. The deconvoluted spectra (Fig. 5) detected: the doublet peaks of Ti 2p as Ti^{4+} ion in TiO_2 oxide (Fig. 5a); the doublet peaks of Nb 3d as Nb^{5+} ion that match to Nb_2O_5 oxide (Fig. 5b); the doublet peaks for Zr 3d as Zr^{4+} ion that correspond to ZrO_2 oxide (Fig. 5c); the deconvoluted peaks of Ta 4f as Ta^{5+} ion that fall to Ta_2O_5 oxide (Fig. 5d);. oxygen peaks for O 1s as O^2, OH^- ions and absorbed H_2O that refer to Ti, Ta, Nb, Zr oxides (Fig. 5e); Therefore, the alloy native passive film is more compact and more resistant than that of Ti, because its composition is formed from a mixture of very protective oxides which reinforced this film.

Returning to Table 3, the lower tendencies to passivation, $|E_{corr} - E_p|$ and passive current densities, j_p were registered, that demonstrate an easier, more rapid passivation, representing more resistant passive film on the alloy surface in comparison with base metal, Ti.

The new Ti-10Nb-10Zr-5Ta alloy presented a superior electrochemical behaviour, because all its electrochemical parameters had more favourable values related to those of Ti.
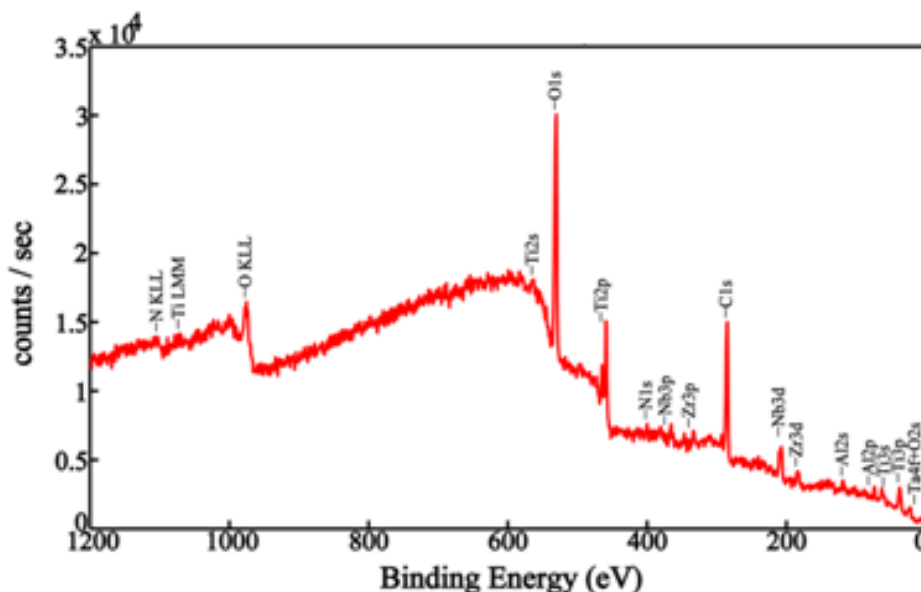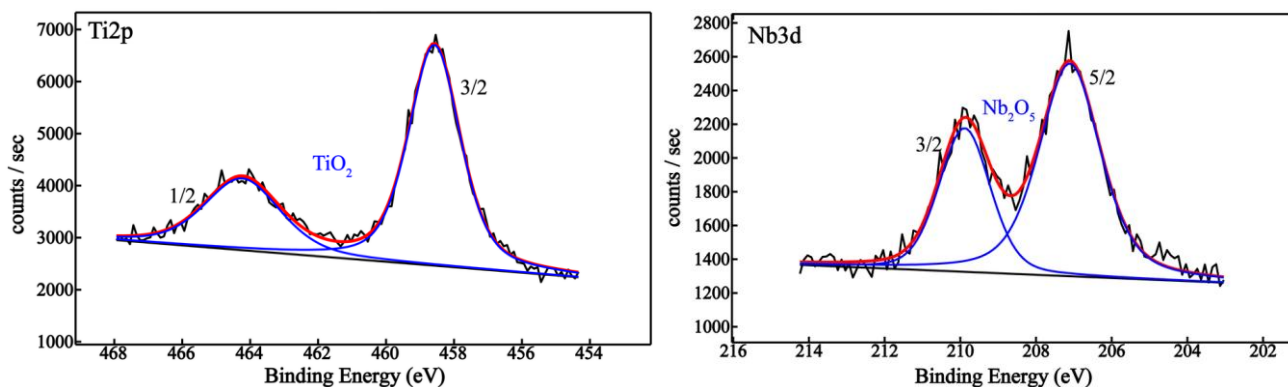

Figure 4. XPS survey spectrum of native passive film on Ti-10Nb-10Zr-5Ta alloy surface.
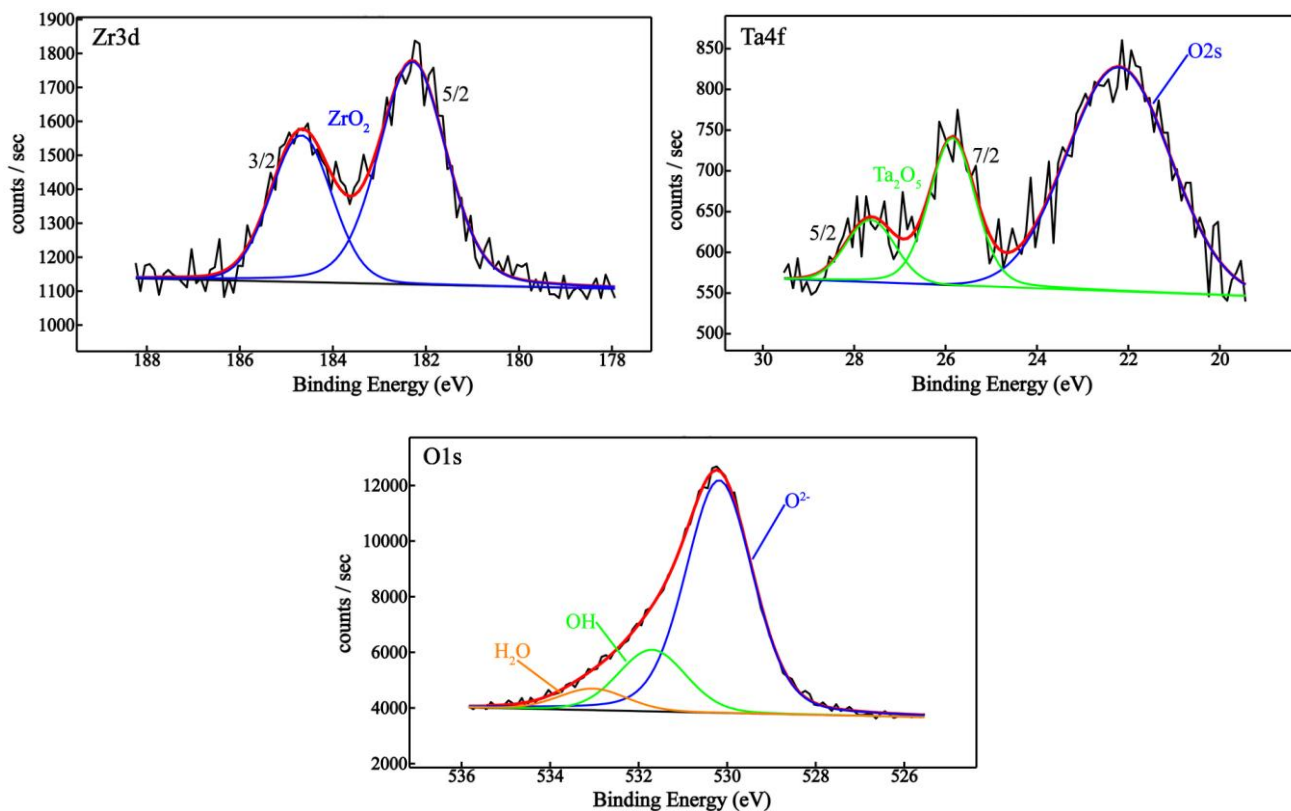
Figure 5. XPS deconvoluted spectra of native passive film on Ti-10Nb-10Zr-5Ta alloy surface.

3.3.2. Alloy corrosion resistance

Table 4. Main corrosion parameters obtained for Ti-10Nb-10Zr-5Ta alloy in comparison with those of Ti in Ringer solutions, at 37^0C

| Material	i_{corr} ($\mu A/cm^2$)	V_{corr} ($\mu m/Y$)	Resistance class	Ion release (ng/cm^2)	R_p ($k\Omega \cdot cm^2$)
Ringer pH = 3.36					
Ti	0.746	8.625	VS	876.30	11.35
Ti-10Nb-10Zr-5Ta	0.421	4.968	VS	504.75	165.13
Ringer pH = 7.58					
Ti	0.724	8.326	VS	845.90	18.25
Ti-10Nb-10Zr-5Ta	0.107	1.263	VS	128.32	230.65
Ringer pH = 8.91					
Ti	1.186	13.700	S	1391.90	13.91
Ti-10Nb-10Zr-5Ta	0.394	4.649	VS	472.34	172.95

VS = Very Stable; S = Stable

The alloy corrosion resistance was appreciated from the linear polarisation measurements using Tafel extrapolation. Main corrosion parameters (excepting polarisation resistance, R_p) from Table 4 revealed significant decreases [22] for the Ti-10Nb-10Zr-5Ta alloy than those of Ti. Corrosion rates,

V_{corr} placed the new alloy in the "Very Stable" resistance class and the corresponding lower ion release rates represent more reduced quantities of ions released into surrounding tissues, namely the decrease of the alloy toxicity in comparison with Ti. Alloy polarisation resistances, R_p had ten times higher values than those of Ti, indicating a more compact, barrier, resistant passive layer (as was shown by XPS analysis). All corrosion parameters prove the higher protective properties of the new alloy compared with those of the base metal, Ti.

3.3.3. Alloy electrochemical behaviour from EIS measurements

Nyquist spectra (Fig. 6) displayed incomplete semicircle with large diameters attributed to capacitive behaviour, passive layer like an insulator; the magnitudes of the diameters and impedances increased from Ti to Ti-10Nb-10Zr-5Ta alloy, namely the alloy presented higher capacitive, passive film [14, 33, 34] being in concordance with the electrochemical results from Figure 3 and Table 3.
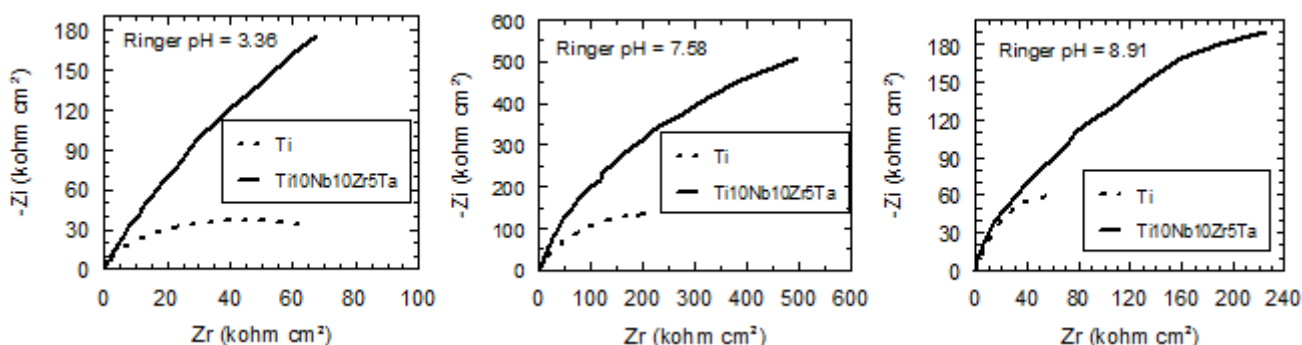

Figure 6. Nyquist spectra for the Ti-10Nb-10Zr-5Ta alloy in comparison with those of Ti in Ringer solutions, at 37^0C.

Bode phase angle spectra (Fig. 7) exhibited two peaks, two phase angles in the low and middle frequency range: the high phase angles had values over -80^0 for the alloy and over -70^0 for Ti, indicative of a capacitive behaviour, a passive film with insulating properties, an inner, barrier layer [14, 27, 28, 35, 36]; the lower phase angles varied around -77^0 for the alloy and around -73^0 for Ti, that reflect a less protective layer, an outer, porous layer [14, 27, 28, 35, 36], separately to the inner, barrier layer. The outer, porous layer is connected with the alloy bioactivity because into its pores can diffuse species from the physiological electrolyte, including phosphorus and calcium ions, that can promote the formation of calcium phosphates or hydroxyapatite, the main inorganic components of the human bone. For the alloy, both high and low phase angles had more favourable values, that denote a more insulating, protective, inner, barrier layer, respectively, a more resistant, outer porous layer, i.e. a nobler behaviour in comparison with that of Ti.
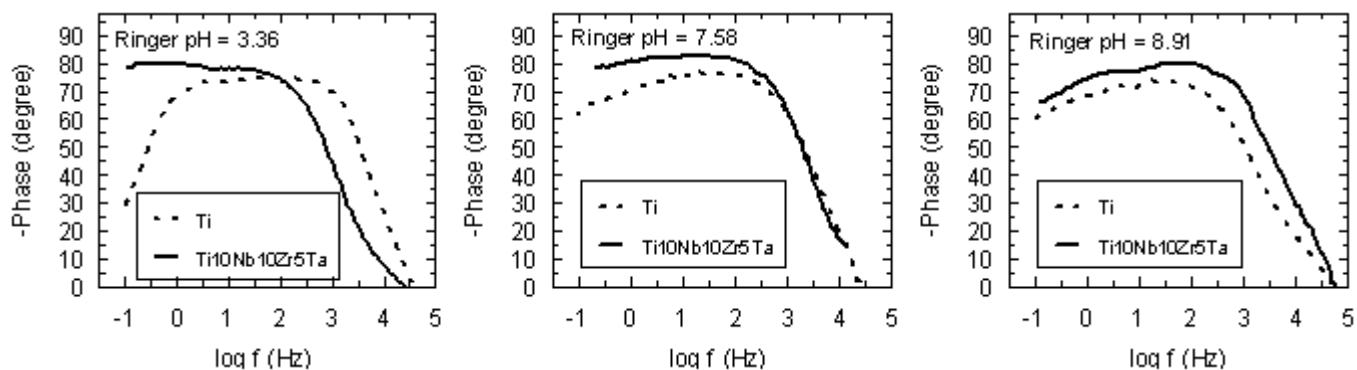
Figure 7. Bode spectra for the Ti-10Nb-10Zr-5Ta alloy in comparison with those of Ti in Ringer solutions, at 37^0C.
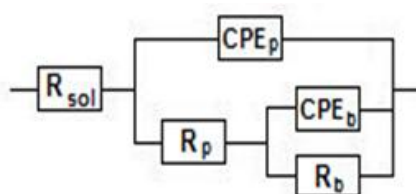
Figure 8. Electric equivalent circuit with two time constants.

Table 5. Fitting parameters for the electric equivalent circuit with two time constants obtained for Ti-10Nb-10Zr-5Ta alloy in comparison with those of Ti in Ringer solutions, at 37^0C.

Material	R_{sol} (Ω cm^2)	R_b (Ω cm^2)	CPE_b (S s^n cm^{-2})	n1	R_p (Ω cm^2)	CPE_p (S s^n cm^{-2})	n2
Ringer pH = 3.36							
Ti	12.60	$5.4\ 10^5$	$9.8\ 10^{-6}$	0.93	$6.9\ 10^3$	$1.3\ 10^{-5}$	0.91
Ti-10Nb-10Zr-5Ta	12.83	6.5×10^6	4.2×10^{-6}	0.94	5.4×10^3	3.6×10^{-5}	0.92
Ringer pH = 7.58							
Ti	12.20	$8.1\ 10^5$	$9.7\ 10^{-6}$	0.94	$7.6\ 10^3$	$1.2\ 10^{-5}$	0.91
Ti-10Nb-10Zr-5Ta	10.79	7.9×10^6	3.0×10^{-6}	0.96	4.6×10^4	1.2×10^{-5}	0.92
Ringer pH = 8.91							
Ti	13.30	$6.2\ 10^5$	$9.9\ 10^{-6}$	0.94	$6.7\ 10^3$	$1.5\ 10^{-5}$	0.92
Ti-10Nb-10Zr-5Ta	10.24	5.4×10^6	5.1×10^{-6}	0.95	1.4×10^4	3.5×10^{-5}	0.92

The those two distinct phase angles predominantly indicate the formation of a passive film with two layers, a bi-layered passive film that was modelled with an electric equivalent circuit with two time constants [33-36] (Fig. 8): the first time constant represents the inner, insulating, barrier layer by its resistance, R_b and capacitance, CPE_b; the second time constant signifies the outer, porous, less protective layer by its resistance, R_p and capacitance, CPE_p (instead of the pure capacitances, constant phase elements, CPE were introduced, relating the surface inhomogeneity, roughness, etc) [28]. The calculated parameters of this equivalent circuit are presented in Table 5: the resistances of the inner layer, R_b had higher values than those of the porous layer, R_p showing that the inner layer is more

insulating, compact and assures the alloy protection; this fact is confirmed by the parameter n1 that has value almost 1, namely, a near ideal capacitor [14]. Comparing the alloy parameters with those of Ti, superior values can be observed, denoting a more resistant, protective, compact passive film existing on the alloy surface.

3.3.4. Alloy long-term behaviour from monitoring of open circuit potentials and corresponding open circuit gradients

The monitoring of the open circuit potentials (Fig. 9) evinced more positive, higher values for Ti-10Nb-10Zr-5Ta alloy in comparison with those of Ti, i.e. a superior resistant passive state as result of the beneficial influence of the alloying elements [37, 38]. All potentials tended to more electropositive values in time, indicating the thickening of the passive film and the improvement of its protective properties [37, 38]. After almost 500 soaking hours, open circuit potentials revealed almost constant levels that show the touching of a stable passive state [37, 38].
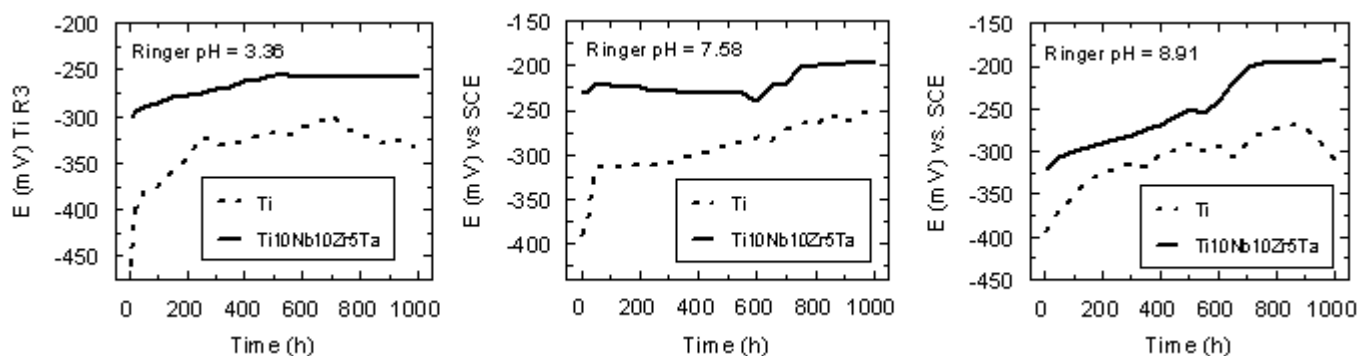

Figure 9. Monitoring of the open circuit potentials for the Ti-10Nb-10Zr-5Ta alloy in comparison with those of Ti in Ringer solutions, at 37^0C.

Table 6. Open circuit potential gradients of Ti-10Nb-10Zr-5Ta alloy in comparison with those of Ti developed in Ringer solutions, at 37^0C.

Material	Time (h)	ΔE_{oc1}(pH) (mV)	ΔE_{oc2}(pH) (mV)	ΔE_{oc3}(pH) (mV)
Ti	0	-98	-57	41
	500	-111	-39	72
	1000	-18	9	27
Ti-10Nb-10Zr-5Ta	0	-70	20	90
	500	-29	-6	23
	1000	-63	-63	-0.4

The open circuit potential gradients (Table 6) had low values (from 0.4 mV to 111 mV) situated under limit of 600 – 700 mV [39-41] and cannot generate galvanic or local corrosion, even in

the case of very large pH differences between 3.36 and 8.91 (ΔE_{oc2}) that could appear on the alloy surface in the "service" conditions.

4. CONCLUSIONS

The new Ti-10Nb-10Zr-5Ta alloy revealed near β fine, homogeneous microstructure. The alloy had superior mechanical properties and low Young's modulus of 63.46 GPa than those of Ti, showing a good resistance to load bearing conditions and no bone atrophy or resorption, assuring a very long "service life time". The new Ti-10Nb-10Zr-5Ta alloy presented a superior electrochemical behaviour, because all its electrochemical parameters had more favourable values related to those of Ti. The alloy native passive film is more compact and more resistant than that of Ti, because its composition is formed from a mixture of very protective oxides (TiO_2, Nb_2O_5, ZrO_2, Ta_2O_5), which reinforced this film. Corrosion rates placed the new alloy in the "Very Stable" resistance class and the corresponding lower ion release rates represent more reduced quantities of ions released into surrounding tissues, namely the decrease of the alloy toxicity in comparison with Ti. Nyquist spectra indicated higher capacitive, protective film for Ti-10Nb-10Zr-5Ta alloy than that for Ti. Bode spectra revealed two phase angles, indicative of a bi-layered passive film that was modelled with an electric equivalent circuit with two time constants: the first time constant represents the inner, insulating, barrier layer and the second time constant signifies the outer, porous, less protective layer. The monitoring of the open circuit potentials evinced more positive, higher values for Ti-10Nb-10Zr-5Ta alloy in comparison with those of Ti, namely, a superior resistant passive state as result of the beneficial influence of the alloying elements.

References

1. E. Eisenbarth, D. Velten, M. Muller, R. Thull and J. Breme, *Biomaterials*, 25 (2004) 5705
2. P. Thomsen, C. Larsson, L. E. Ericson, L. Sennerby, J. Lausama and B. Kasemo, *J. Mater. Sci. Mater. Med.*, 8 (1997) 653
3. Y. Okazaki, Y. Ito, K. Kyo and T. Tateishi, *Mater. Sci. Eng. A*, 213 (1996) 138
4. Y. Okazaki, S. Rao, Y. Ito and T. Tateishi, *Biomaterials*, 19 (1998) 1197
5. S. Y. Yu and J. R. Scully, *Corrosion,* 53 (1997) 965
6. J. A. Davidson, A. K. Mishra, P. Kovacs and R. A. Poggie, *Bio-Med. Mater. Eng.*, 4 (1994) 231
7. Y. Okazaki, E. Nishimura, H. Nakada and K. Kobayashi, *Biomaterials*, 22 (2001) 599
8. Y. Okazaki, *Curr. Opin. Solid State Mater. Sci.,* 5 (2001) 45
9. P. K. Zysett, X. E. Guo, C. E. Hoffler, K. E. Moore and S. A. Goldstein, *Tech. Health Care*, 6 (1998) 429

10. R. Banerjee, S. Nag, J. Stechschulte and H. L. Fraser, *Biomaterials*, 25 (2004) 3413
11. Y. Tanaka, M. Nakai, T. Akahori, M. Niinomi, Y. Tsutsumi, H. Doi and T. Hanawa, *Corros. Sci.*, 50 (2008) 2111
12. A. Fukuda, M. Takemoto, T. Saito, S. Fujibayashi, M. Neo, S. Yamaguchi, T. Kizuki, T. Matsushita, M. Niinomi, T. Kokubo and T. Nakamura, *Acta Biomater.*, 7 (2011) 1379
13. S. J. Li, R. Yang, M. Niinomi, Y. l. Hao and Y. Y. Cui, *Biomaterials*, 25 (2004) 2525
14. M. Karthega, V. Raman and N. Rajendran, *Acta Biomater.*, 3 (2007) 1019
15. T. Kasuga, M. Nogami, M. Niinomi and T. Hattori, *Biomaterials*, 24 (2003) 283
16. L. Zhao, Y. Wei, J. Li, Y. Han, R. Ye and Y. Zhang, *J. Biomed. Mater. Res. A*, 82A (2010) 432
17. E. B. Taddei, V. A. R. Henriques, C. R. M. Silva and C. A. A. Cairo, *Mater. Sci. Forum*, 498-499 (2005) 34
18. E. B. Taddei, V. A. R. Henriques, C. R. M. Silva and C. A. A. Cairo, *Mater. Res.,* 10 (2007) 289
19. R. Van Noort, *J. Mater. Sci.*, 22 (1987) 3801
20. Z. Cai, H. Nakajima, M. Woldu, A. Berglund, M. Bergman and T. Okabe, *Biomaterials,* 20 (1999) 183
21. C. Fonseca and M. A. Barbosa, *Corros. Sci.*, 43 (2001) 547
22. T. Spataru, N. Spataru, *J. Hazard. Mater.,* 180 (2010) 777
23. I. Ramires, A. C. Guastaldi, *Quim. Nova*, 25 (2002) 10
24. T. Spataru, M. Marcu, A. Banu, E. Roman, N. Spataru, *Electrochim. Acta*, 54 (2009) 3316
25. E. Vasilescu, P. Drob, D. Raducanu, I. Cinca, D. Mareci, J. M. Calderon Moreno, M. Popa, C. Vasilescu and J. C. Mirza Rosca, *Corros. Sci.*, 51 (2009) 2885
26. V. D. Cojocaru, D. Raducanu, I. Cinca, E. Vasilescu, P. Drob, C. Vasilescu and S. I. Drob, *Mater. Corros.*, 64 (2013) 500
27. V. A. Alves, R. Q. Reis, I. C. B. Santos, D. G. Souza, T. de F. Goncalves, M. A. Pereira-da-Silva, *Corros. Sci.,* 51 (2009) 2473
28. T. Spataru, M. Marcu, A. Banu, E. Roman, N. Spataru, Rev. Chim. (Buch.) 59 (2008) 1366
29. M. V. Popa, E. Vasilescu, P. Drob, C. Vasilescu, S. I. Drob, D. Mareci, J. C. Mirza Rosca, *Quim. Nova*, 33 (2010) 1892
30. M. Niinomi, *J. Mech. Behav. Biomed. Mater.*, 1 (2008) 30
31. J. F. Moulder, W. F. Stickle, P. E. Sobol and K. D. Bomben, *Handbook of X-ray photoelectron spectroscopy*, Physical Electronics USA, Inc., Chamhassen, 1995
32. A. V. Naumkin, A. Kraut-Vass, S. W. Gaarenstroom and C. J. Powell, *NIST X-ray photoelectron spectroscopy database*. NIST standard reference database 20, version 4.1, US Secretary of Commerce on behalf of the United States of America, 2012
33. S. L. Assis, S. Wolynec and I. Costa, *Mater. Corros.*, 59 (2008) 739
34. A. Robin, O. A. S. Carvalho, S. G. Schneider and S. Schneider, *Mater. Corros.*, 59 (2008) 929
35. S. L. Assis and I. Costa, *Mater. Corros.*, 58 (2007) 329
36. B. L. Wang, Y. F. Zheng and L. C. Zhao, *Mater. Corros.*, 60 (2009) 788
37. J. Black, *Biological performance of materials: Fundamentals of biocompatibility*, M. Decker Inc. New York, 1992
38. D. J. Blackwood, A. W. C. Chua, K. H. W. Seah, R. Thampuran and S. H. Teoh, *Corros. Sci.*, 42 (2000) 481
39. Q. Guo, M. Du and C. Zhou, *Proceedings of 16th International Corrosion Congress*, Sept. 2005, Beijing, China, paper 08-28
40. C. Sola, A. Amorim, A. Espias, S. Capelo, J. Fernandes, L. Proenca, L. Sanchez and I. Fonseca, *Int. J. Electrochem. Sci.*, 8 (2013) 406
41. E. Blasco-Tamarit, A. Igual-Munoz, J. Garcia Anton and D. M. Garcia-Garcia, *Corros. Sci.*, 51 (2009) 1095